Alpha Lab Report
Radiation, Protection, Dosimetry and Detectors SH2603

Konstadinos Papadhopuli, Federico Pati

February 11, 2026

Contents

1 Introduction

This laboratory exercise focuses on the study of alpha decay and spontaneous fission, two processes that play a vital role in the field of nuclear energy engineering. Alpha decay involves the emission of alpha particles (helium nuclei) from unstable atomic nuclei, which results in a decrease in the atomic number and mass of the parent nucleus. This process is prevalent in heavy isotopes, such as californium-252 (Cf-252), which can also undergo spontaneous fission, an alternative decay mode in which the nucleus splits into two or more smaller nuclei along with the release of neutrons.

This laboratory experiment utilizes a triple-alpha source containing isotopes of curium-244 (Cm-244), americium-241 (Am-241) and plutonium-239 (Pu-239) in order to calibrate the detector and accurately measure the alpha particle energies. Firstly, by investigating the energy loss of the alpha particles in the air as a function of pressure, we calculated the range of the alpha particles in the air. The range of a particle is the distance it travels through a material before losing all its energy and coming to a stop. This range depends on the particle's energy, type, and the properties of the material it traverses. Afterwards, we analyzed the spectrum of an unknown alpha source, and finally we measured the fragment energies from the spontaneous fission of Cf-252. In particular, the fraction of atoms that undergo α-decay and the fraction of spontaneous fission will be analyzed. This fraction is known as branching ratio, it is the probability of a radioactive decay process resulting in a particular decay mode among multiple possible decay paths.

2 Theory

2.1 Alpha Decay and Spontaneous Fission

Alpha decay involves the spontaneous emission of an alpha particle from an atomic nucleus. If the initial nucleus (usually called the mother nucleus) has mass number A, N neutrons, and Z protons, the product left after alpha particle emission (the daughter nucleus) has mass number A=4, proton number Z-2, and neutron number N-2 [1][3]. Several naturally occurring isotopes decay by alpha emission. Frequently, the daughter nucleus of an alpha decay is radioactive as well, leading to the following β-decay that produces an isotope that can be α radioactive itself. Therefore, the chain of decays formed is called a radioactive decay series. The four series of radioactive decay can be seen in Fig.1. The triple alpha source used in this experiment consists of the following isotopes: ^{244}Cm , ^{241}Am, ^{239}Pu . As we can see in Fig.1, these three isotopes decay into a daughter nucleus by emitting an alpha particle as shown below [3]:

- $^{244}\text{Cm} \rightarrow {}^{240}\text{Pu} + \alpha$ with $Q_\alpha = 5.804$ MeV
- $^{241}\text{Am} \rightarrow {}^{237}\text{Np} + \alpha$ with $Q_\alpha = 5.485$ MeV
- $^{239}\text{Pu} \rightarrow {}^{235}\text{U} + \alpha$ with $Q_\alpha = 5.156$ MeV

where Q_α is the energy of the alpha particle emitted in the decay.

In the case of some heavy isotopes that are neutron-rich, another decay mode, spontaneous fission, is strong enough to compete with alpha decay. In this process, the nucleus deforms and is separated into two large parts, called fission products. Usually, a number of neutrons are also released in the process (2-3).

2.2 The Interaction of Charged Particles in Matter

A heavy charged particle that enters a material will immediately start to interact with the negatively charged electrons and the positively charged atomic nuclei. The major part of the energy loss will occur through the interaction with electrons. Therefore, due to the large

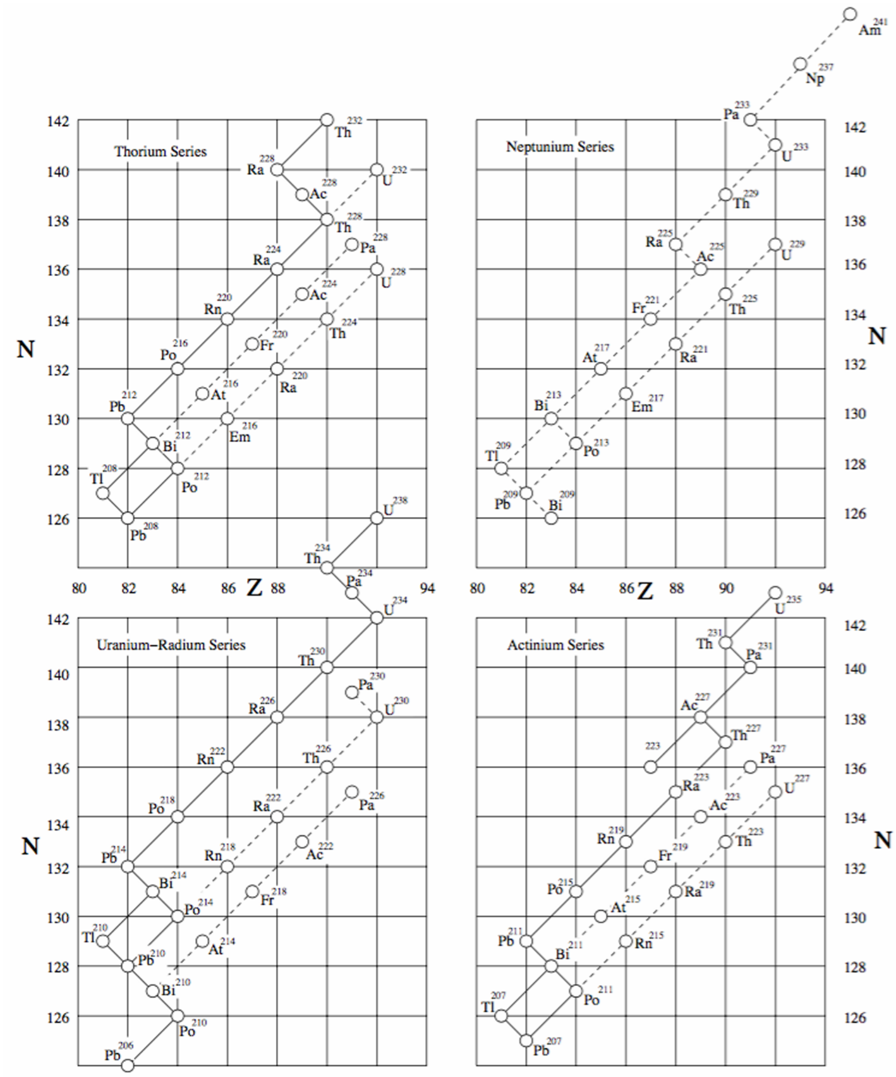

Figure 1: The four radioactive decay series of the heavy elements. Solid lines indicate naturally occurring decays, while dashed lines indicate decays from artificially produced radioactive isotopes[3].

number of interactions between the particle and the electrons, and due to the statistical nature of the interaction, we can assume that the energy loss of the particle as a continuous quantity. This is expressed in terms of the stopping power, written $\frac{dE}{dx}$, where E is the energy of the particle, and x is the penetration depth into the material. The energy loss per travelled length (stopping power) , is given by the Bethe-Bloch formula[1]:

$$-\frac{dE}{dx} = \left(\frac{e^2}{4\pi\epsilon_0}\right)^2 \frac{4\pi z^2 N_a Z\rho}{m_e c^2 \beta^2 A}\left[\ln\left(\frac{2m_e c^2\beta^2}{I}\right) - \ln(1-\beta^2) - \beta^2\right] \tag{1}$$

where $v = \beta \cdot c$ is the velocity of the particle, z is its proton number, Z, A, and ρ are the atomic number, atomic weight, and mass density of the material. N_a is Avogadro's number, m_e is the electron mass, and I is the mean excitation energy of the atomic electrons in the stopping material.

When plotting the stopping power as a function of the penetration depth we get the Bragg curve. The final penetration depth of the particle is called the range of the alpha particle and it is found at the end of the Bragg curve (intercept with x-axis).

2.3 Ionization Chamber

When an atomic electron gets energized and eventually leaves its position in the electron shell it is said that the atom is ionised. When this process takes place in a gas inside a container ions and free electrons are created, which can be transported by placing a strong electrical field inside the container. Therefore, it is possible to collect the charges, creating that way an electric pulse that can be amplified and then recorded. The pulse can be amplified by increasing the voltage of the electric field inside the container which will lead to a series of second ionization, by the free electrons travelling through the gas, creating the so called cascade of ion-electron pars. This is the basic principle of an ionization chamber that we used in this lab experiment and is shown in Fig.2.

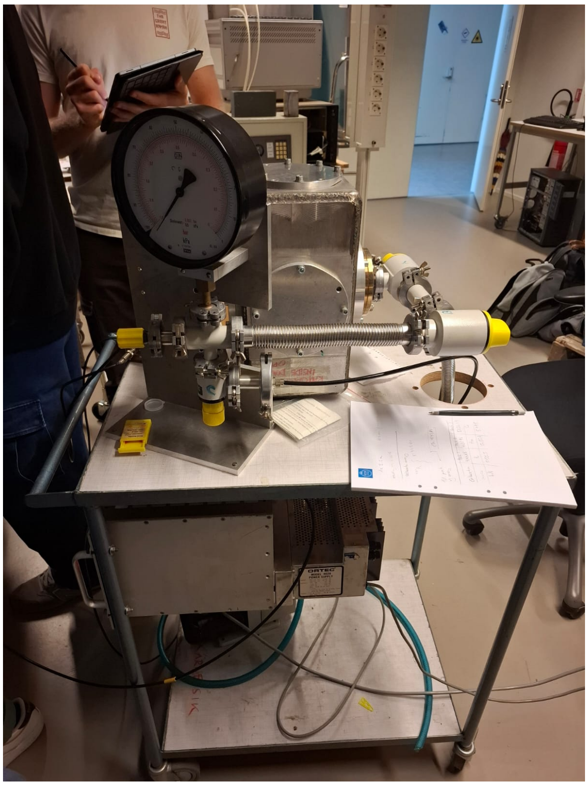

Figure 2: The ionization chamber detector used in this lab experiment

3 Experimental Setup

In this lab experiment we used two ionization chamber detectors. In order to measure the energy loss of alpha particles and calculate their range, the air between the source and the detector was removed since heavy charged particles have a limited range in air at atmospheric pressure. A schematic picture of the setup is shown in Fig.3. We can alternate between the source we want to work with without breaking the vacuum by pushing/pulling or rotating a rod that is mounted in the large chamber. In this way, the source of interest is put in front of the collimator and the detector is then shielded from the other one. Moreover, we can control the air pressure used in the experiment through a valve (Valve D as shown in Fig.3) that is located in the the small vacuum chamber. After making sure that we have atmospheric pressure we opened the small vacuum chamber and investigated the source and the Si surface barrier that is used in both detectors. The electric pulse from the Si detector are amplified and shaped by the preamplifier and main amplifier modules, which can be set at a high and a low gain depending on the energy ranges of particles detected, and subsequently digitised and stored by a multi-channel analyser (MCA) card residing in a PC. The multichannel analyzer is shown in Fig.4.

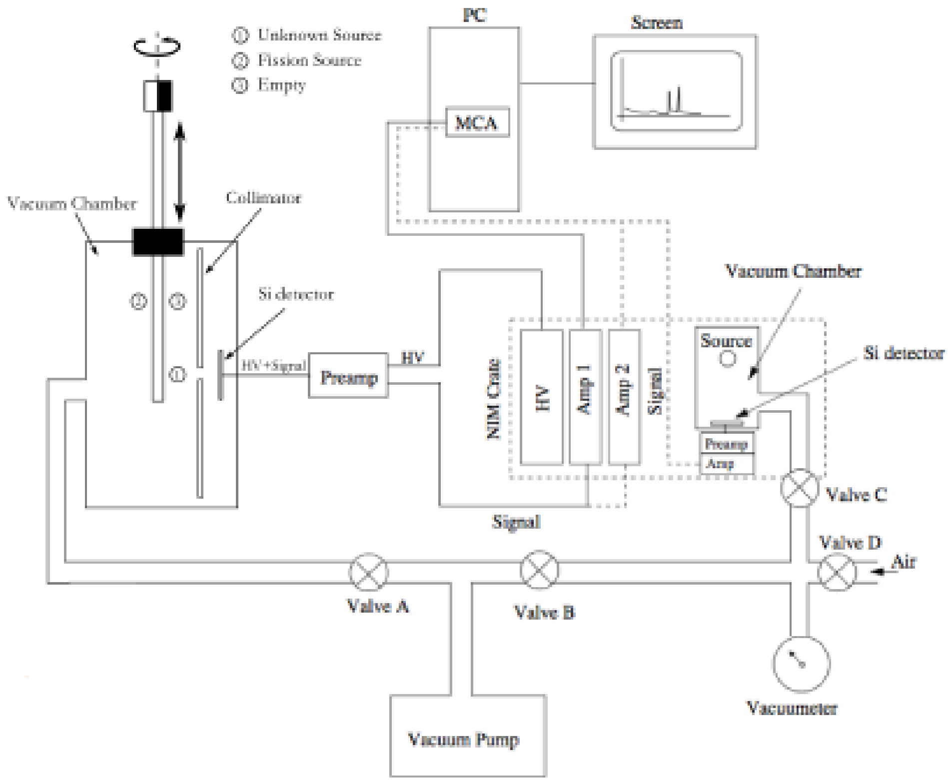

Figure 3: A schematic view of the two vacuum chambers and the electronics for energy measurements of alpha particles and fission fragments.[3]

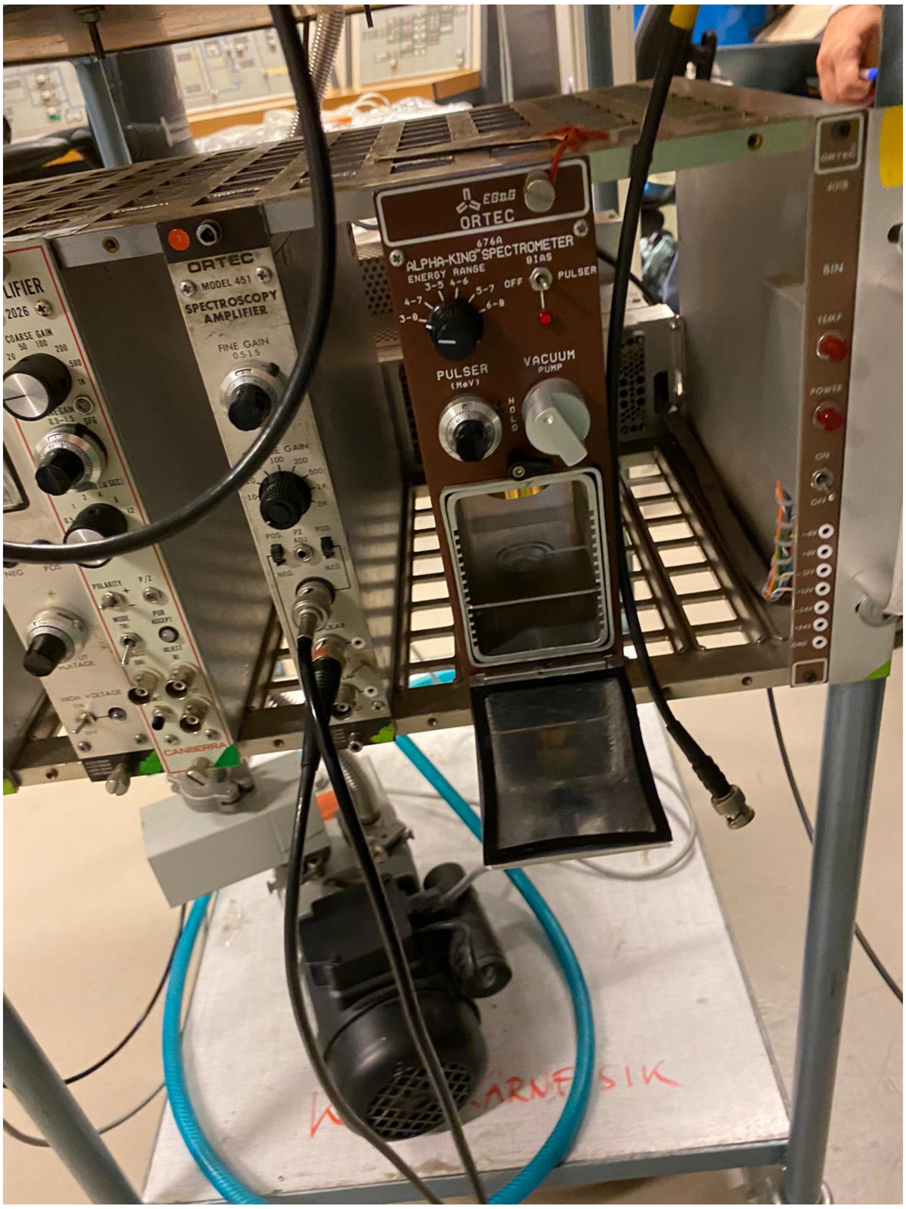

Figure 4: Multichannel analyzer

4 Results

4.1 Determination of the Range of Alpha Particles in Air

At the first part of the experiment we determined the range of alpha particles in the air by adjusting the air pressure from the valve shown in Fig.3. Before obtaining the measurements, we calibrated the detectors using the known alpha particle energies of the decay of the triple alpha source (^{244}Cm, ^{241}Am, ^{239}Pu). Therefore, we placed the source inside the vacuum chamber and measured the distance from the source to the detector which was $d = 3.2$ cm. Then, we obtained the spectrum shown in Fig.5 using the TUKAN software, setting the time of measurement to $t = 5$ minutes.

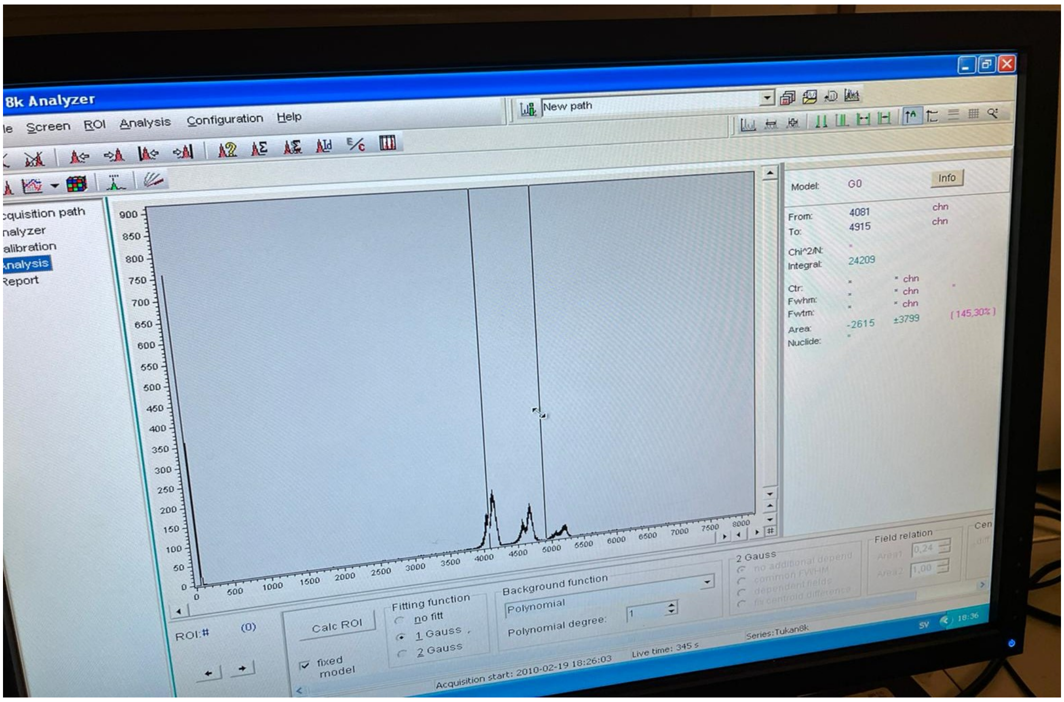

Figure 5: The spectrum of the triple alpha source obtained from TUKAN software

Using the known energies of the alpha particles ($Q_/alpha$) emitted in the decay of the triple alpha source we calibrated the detector in order to conduct the next phases of the experiment with accurate measurements.

In order to determine the range of the alpha particles in air we will obtain measurements of the energy of alpha particles as a function of the air pressure between the source and the detector. Afterwards, using the ideal gas law

$$PV = nRT \tag{2}$$

since the temperature T is constant throughout the experiment we can express the equilibrium through the product of pressure and volume

$$P_{atm}V_{atm} = PV_x \tag{3}$$

where P_{atm} and V_{atm} is the atmospheric pressure and volume at atmospheric pressure respectively. Moreover, since the volume of the area between the source and the detector is

$$V_x = A \cdot x \tag{4}$$

replacing eq. 4 in eq.3, we can write the penetration depth of the particle as a function of the pressure

$$x = \frac{P}{P_{atm}} \cdot d \tag{5}$$

where d is the measured distance of the source from the detector (d = 3.2 cm), P_{atm} is the atmospheric pressure and P is the pressure adjusted through the valve, changing in every measurement. Therefore, since every parameter and variable of 5 is known we can calculate the distance x which is the penetration depth of the alpha particle under atmospheric pressure.

We obtained 8 measurements of the spectrum of the triple alpha, by increasing the pressure of the air between the source and the detector each time.The measuring time was set to 5 minutes and the results are shown in Table 1.

Table 1: The energy of the alpha particles for each peak in relation to the air pressure in each measurement and the calculated penetration depth.

		Energy of alpha particles [keV]		
Penetration Depth [cm]	**Pressure [KPa]**	Peak 1	Peak 2	Peak 3
0	0	5155.5	5485.7	5798
0.300025	9.5	4798.05	5133.75	5457.08
0.679003	21.5	4358.57	4723.07	5051.67
0.947446	30	4113.68	4482.74	4809.59
1.263262	40	3815	4185	4615
1.579077	50	3444.88	3851.73	4215.6
1.894893	60	3113.23	3471.26	3901
2.210708	70	-	3184.17	3593.56

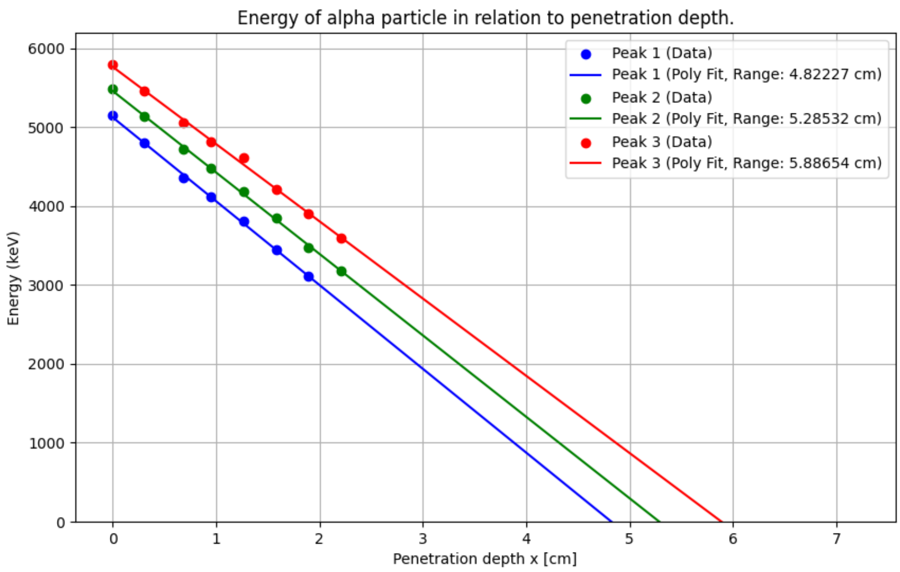

Figure 6: Energy of alpha particles as a function of the penetration depth for the three different peaks according to the three different isotopes of the triple alpha source. The range of particles for the different isotopes are presented in the label of the figure

As shown in Fig. 6, the penetration depth of the alpha particles increases as the air pressure between the source and the detector decreases. This is expected because, with lower air pressure, there are fewer atoms for the alpha particles to interact with, allowing them to penetrate the air to greater depths. The range of the alpha particles emitted from the decay of each isotope in the triple alpha source is also shown. This range was calculated as the magnitude of the interception point of the polynomial fit of the data with the x axis. The range for the three different isotopes are presented in Table 2.

Table 2: The range the alpha particles for each peak corresponding to the alpha particles emitted from the decay of the three different isotopes of the triple alpha source.

Range x [cm]		
Peak 1 (Plutonium-239)	Peak 2 (Americium-241)	Peak 3 (Curium-244)
4.82227	5.28532	5.88654

We can see from Table 2 that the range of the alpha particles decreases for decreasing initial energies of the alpha particle. This is logical as an alpha particle with a high initial energy has a greater penetrative power than an alpha particle with lower initial energy.

Furthermore, $\frac{dE}{dx}$ was calculated by applying the following formula on the data points of Fig.6:

$$\left.\frac{dE}{dx}\right|_{x_i} \approx \frac{E(x_{i+1}) - E(x_i)}{x_{i+1} - x_i} \tag{6}$$

The calculated expression corresponds to the middle point of x_{i+1} and x_i. Finally, a spline function was used to plot Fig.7. The uncertainties in Fig.6 and Fig.7 are very small so that the error bars practically not observable.

In Fig.7 we can see the Bragg-curve of the alpha particles for the three isotopes.

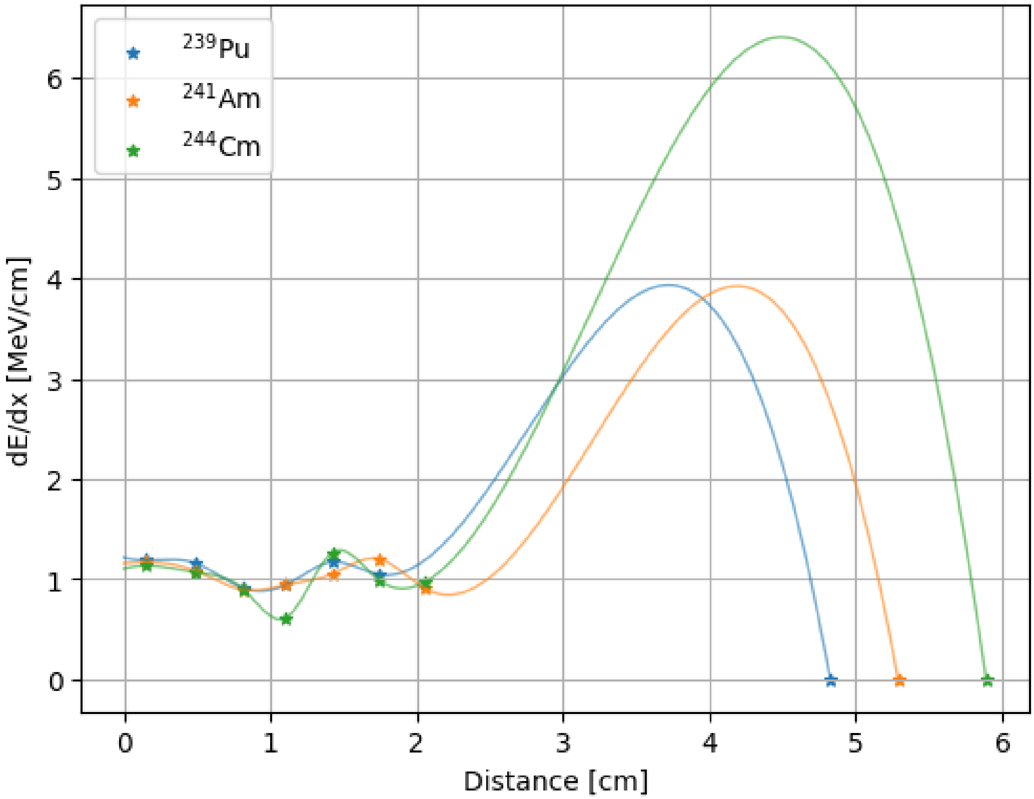

Figure 7: The stopping power $\frac{dE}{dx}$ as a function of the penetration depth x. The curves that are shown in the figure are the Bragg-curve of the alpha particle from each isotope of the triple alpha source.

4.2 Unknown Source

In the second part of the experiment, we try to trace back to the emitting radionuclide, by comparing the energy peaks of the emitted α-particle, to the one listed in the Live Chart of Nuclides from IAEA.[2]

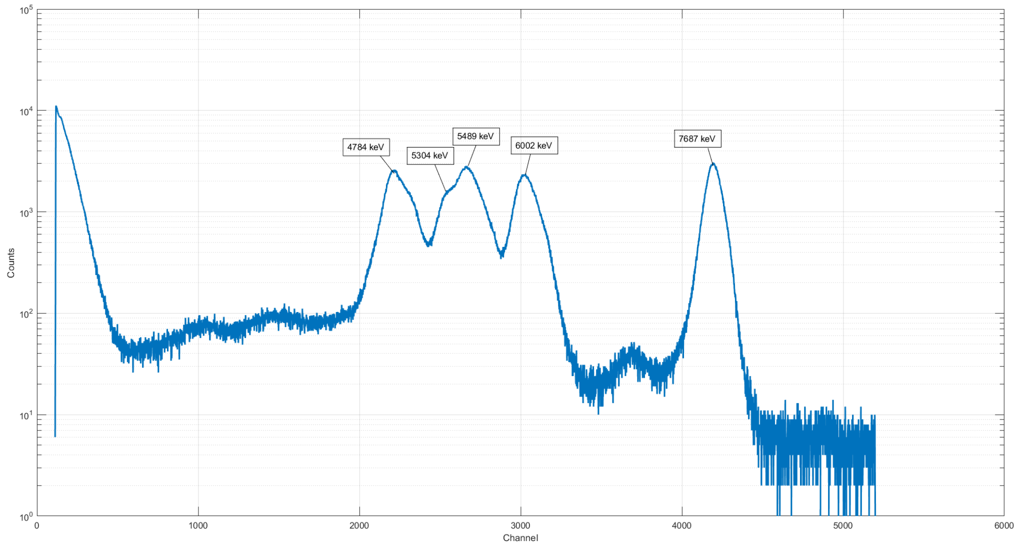

Figure 8: Energy spectrum of the unknown alpha emitter

The detected energies, the corresponding isotopes, and the energy according to IAEA are listed in Table 3. As we can see, all of the measured peaks correspond with good accuracy to one of their corresponding isotopes.

Table 3: Energy of the unknown nuclide compared with the corresponding isotope.

Energy peak measured [keV]	**Corresponding isotope**	**Energy of the isotope**
4784	^{226}Ra	4784.3
5304	^{210}Po	5304.38
5489	^{222}Rn	5489.38
6002	^{218}Po	6002.55
7687	^{214}Po	7686.82

4.3 Spontaneous Fission

In the last part of this report we will analyze the phenomena of spontaneous fission. Now, the radioactive source is ^{252}Cf, a nuclide that is subjected to α-decay and spontaneous fission.

After a measurement time of 40h, the new energy spectrum is represented in Figure 9.

In this plot, three different peaks are evident. The first one is due to the decay and emission of the α particle, and the second and the third peaks are caused by the fission fragments of the spontaneous fission.

Our next aim is to evaluate the branching ratio. The branching ratio is the fraction of all decay or reaction events that follow a specific decay channel. It represents the probability of a particular outcome among all possible outcomes in a process.

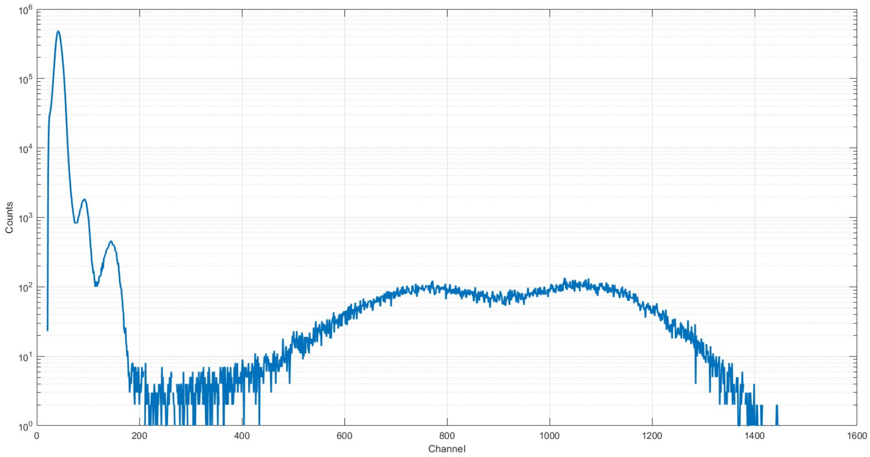

Figure 9: Energy spectrum of ^{252}Cf

The equation used to calculated are reported below:

$$BR_\alpha = \frac{A_\alpha}{A_\alpha + A_{fiss}/2} \qquad BR_{fiss} = \frac{A_{fiss}/2}{A_\alpha + A_{fiss}/2}$$

Where A_α and A_{fiss} are the area respectively below alpha and fission events in the energy spectrum in Figure 9. The area of spontaneous fission is divided by two because each event cause the formation of two fission fragments. To compute this value, first of all we are interested in dividing the two possible events.

For what concerns the alpha particle, the area between channel 1 and 180 is evaluated by adding the counts of each channel. While, for the fission fragments the area is evaluated summing value between 500 e 1300.

The results are reported in Table 4:

Table 4: Area and the resulting branching ratio for these events.

Event	Area [counts]	Branching Ratio [%]	BR [%] from IAEA
Alpha	7'218'910	99.63	96.898
Fission	53'403	0.37	3.102

Comparing this value with the reference from IAEA [2] we can notice a significant difference: the branching ratio for the spontaneous fission is an order of magnitude smaller. This could only be explained assuming that Cf-252 is not in pure state in the sample. It's easy to expect that an other isotope of californium (Cf-250) is in the source since it is very difficult to separate. The branching ratio of Cf-250 are:

$$BR_\alpha(^{250}\text{Cf}) = 99.923\% \qquad BR_{fiss}a(^{250}\text{Cf}) = 0.077\%$$

These result are more similar to the one obtained, so it seems that both of them are present in the sample. This was expected also by the presence of three peaks in the alpha-decay, while Cf-252 should have only two. Furthermore, another point that validates this theory is the half-life:

$$t_{\frac{1}{2}}(^{250}\text{Cf}) = 13.04y \qquad t_{\frac{1}{2}}(^{252}\text{Cf}) = 2.647y$$

Since Cf-250 has a longer half-time, it is reasonable to expect that the source is aged and the amount of Cf-252 is sensibly reduced.

Other analysis could be carried on considering only the alpha peak that belongs to source of our interest, but since we don't have information on the energy or the concentration, we conclude the analysis here.

4.4 Validity of results

Even if not included in given data, errors are always present even in the second and third lab experience. Several sources of uncertainty may arise and some of them may regards the detector resolution, its dead time and its proper calibration . Moreover, we should consider the background radiation from the environment or from other sources in the lab. Also, dealing with alpha particles, discrepancy from theoretical solution may arise due to the thickness of the sample: the radiation may lose energy as they travel through the material in a process known as self absorption. All these factor may lead to some errors, however, for our purpose these variation from the exact value are negligible, without influencing in a relevant way the results.

5 Conclusions

In conclusion, this laboratory exercise successfully demonstrated the principles of alpha decay and spontaneous fission. We successfully used a surface barrier detectors and two vacuum chambers in order to obtain the energy spectrum of alpha particles and fission fragments. Moreover, we determined the range of alpha particles in air by adjusting the pressure of the air inside the chambers. The experimental data we acquired are in strong accordance with the theoretical data.

For the second part, we analyzed an alpha spectrum of an unknown source, determining all the alpha emitters thanks to their energy peaks. Finally, we studied the energy spectrum of californium-252. Here, the source seemed to be known, but the evaluation of the branching ratio reveals that the source wasn't pure. The age of the source and the presence of Cf-250 during manufacturing suggest that Cf-252 constitutes only a minor fraction of the sample.

References

[1] Torbjörn Bäck. Radiation protection, dosimetry, and detectors compendium, September 5, 2023 (version 1.9).

[2] IAEA. Livechart - Table of Nuclides - Nuclear structure and decay data — www-nds.iaea.org. https://www-nds.iaea.org/relnsd/vcharthtml/VChartHTML.html. [Accessed 23-09-2024].

[3] J. E. Turner. *Atoms, radiation, and radiation protection.* Wiley-VCH, 2007.